HHS Public Access

Author manuscript

Microcirculation. Author manuscript; available in PMC 2021 August 01.

Published in final edited form as:

Microcirculation. 2020 August ; 27(6): e12621. doi:10.1111/micc.12621.

INDIVIDUAL CELL MOTION IN HEALTHY HUMAN SKIN MICROVASCULATURE BY REFLECTANCE CONFOCAL VIDEO MICROSCOPY

Inga Saknite[1], **Zijun Zhao**[1,2,3], **J. Randall Patrinely**[1,2,3], **Michael Byrne**[4,5], **Madan Jagasia**[4,5], **Eric R. Tkaczyk**[1,2,5,6]

[1]Vanderbilt Dermatology Translational Research Clinic, Department of Dermatology, Vanderbilt University Medical Center, Nashville, TN, USA

[2]Dermatology Service and Research Service, Tennessee Valley Healthcare System, Department of Veterans Affairs, Nashville, TN, USA

[3]Vanderbilt University School of Medicine, Nashville, TN, USA

[4]Division of Hematology/Oncology, Department of Medicine, Vanderbilt University Medical Center, Nashville, TN, USA

[5]Vanderbilt-Ingram Cancer Center, Nashville, TN, USA

[6]Department of Biomedical Engineering, Vanderbilt University, Nashville, TN, USA

Abstract

Objective—Describe upper dermal microvasculature of healthy human skin in terms of density and size of cutaneous blood vessels, leukocyte velocity, and leukocyte interactions with the endothelium.

Methods—We used a reflectance confocal microscope, the VivaScope 1500, to acquire videos of individual cell motion.

Results—We found no rolling leukocytes in the upper microvasculature of ten healthy subjects. We observed “paused” leukocytes i.e. leukocytes that temporarily stop, coinciding with the simultaneous stopping of the rest of the blood flow. We imaged more paused (median: 1.0 per subject) and adherent (1.5) leukocytes in the forearm than in the chest (median 0 paused and 0 adherent per subject) per 5 minutes of videos per body site. Leukocytes were paused for a median of 7 seconds in the forearm and 3 seconds in the chest, and we found no correlation of this parameter to the blood vessel or leukocyte size. We visualized blood flow change direction. Flowing leukocyte velocities followed a log-normal distribution and were on average higher in the chest (117 μm/sec) than in the forearm (66 μm/sec).

Corresponding Author: Inga Saknite, PhD, Address: One Hundred Oaks, 719 Thompson Lane, Suite 26300, Nashville, TN 37204, Phone: (615) 936-4624; Fax: (615) 343-3947, inga.saknite@vumc.org.

This study was conducted within the Department of Dermatology, Vanderbilt University Medical Center. Address: One Hundred Oaks, 719 Thompson Lane, Suite 26300, Nashville, TN 37204, USA.

Conclusions—The proposed method and reported values in healthy skin provide new insights into intact human skin microcirculation.

Keywords

rolling; adhesion; leukocyte; confocal; noninvasive; paused leukocyte

INTRODUCTION

Cutaneous microcirculation regulates the exchange of nutrients, heat and inflammatory cells between blood and tissue, and plays a significant role in many diseases, including cancer and hypersensitivity reactions.[1] Our understanding of human cutaneous microcirculation has been improved by noninvasive optical technologies, advancing the development of imaging biomarkers for angiogenic cancers, e.g. melanoma,[2] cardiovascular disease,[3] and inflammatory disease, e.g. psoriasis.[4] Laser doppler flowmetry, laser speckle imaging and optical coherence tomography[5] enable measurement of blood flow velocity, but are limited to the assessment of bulk tissue. Visualization of individual cell motion in a single cutaneous blood vessel may further enhance our understanding of disease pathology and enable the development of novel biomarkers.

Human cutaneous microcirculation is characterized by an upper (near the dermal-epidermal junction, DEJ) and lower (near the dermal-subcutaneous junction) horizontal plexus,[6–8] or a tree-like branching network.[9] To deliver the necessary nutrients and cells to the topmost layers of skin, terminal arterioles, 17–26 μm in diameter,[10] become capillaries with an external diameter of 8–12 μm[10,11] and an internal diameter of 4–6 μm.[10] Capillaries then merge and form post-capillary venules, 18–23 μm in external and 10–15 μm in internal diameter.[6] By volume, blood consists mainly of plasma (~54%), red blood cells (~45%), and leukocytes and platelets (~1%). By count, ~ 94% of the cells in a healthy cutaneous blood vessel are red blood cells (RBCs), whereas the rest are platelets (~ 5.9 %) and leukocytes (.09%). RBCs are ~1.7–2.2 μm thick biconcave disks ~7.5–8.7 μm in diameter,[12] and the diameter of platelets ranges from 2–4 μm.[13] Undeformed human leukocytes are spherical cells with diameters in the range of 4–8 μm (lymphocytes), 5–8 μm (neutrophils), 4–10 μm (monocytes), and 6–8 μm (eosinophils).[14–16] On a blood smear, for comparison, leukocyte is deformed to a pancake-shape[15] with diameter ranging from 6–20 um[17] (Table 1). RBCs and leukocytes are highly deformable and can squeeze through a narrow vessel.[18] Without a sufficient pressure gradient, it can take up to 10–20 seconds[19] for a leukocyte to squeeze through a capillary smaller than its unstressed diameter.[20,21] This process is variably termed leukocyte “pausing,”[20] “plugging,”[20,22–35] “stopping,”[28,30,34,36,37] “trapping”[21,23–25,28,30,31,34,35] and “retention”.[22,25,28,31,34,35,37] This has been previously observed in the blood vessels of myocardium,[22,23,28,32,34,35] cremaster[24,25] and skeletal muscle,[26,33] lungs,[38] and eyes[20,27,29–31,36] in a broad range of animal species (rats,[22,26,28,31,34,35] dogs,[23,32] hamsters,[24,25,33] rabbits,[29,36,38] and monkeys[30,36]) with most leukocytes temporarily stopping for <1 second. Although with no mention of leukocyte involvement, RBC velocity drop to 0 μm/sec for up to 10 seconds[21,39], as well as blood flow change direction[39] has been observed in human nailfold capillaries.

Normal microvascular function is ensured by a pressure gradient across the blood vessel, which affects fluid filtration and flow rate, and is impaired in microvascular disorders such as Raynaud's phenomenon, lymphedema, and diabetes.[21] Compared to vessels >70 μm in diameter where blood can be treated as a homogenous suspension, flow in the microvasculature is increasingly influenced by the shear forces developed at the vessel wall.[40] Because leukocytes are larger in volume, spherical in shape, and less easily deformed than RBCs, they tend to flow slower than RBCs in capillaries.[41] When a leukocyte passes through a narrow capillary, it temporarily blocks the rest of the flow, leading to an accumulation of RBCs behind it ("a queue of cells").[42] As the capillary widens to a postcapillary venule, the faster flowing RBCs push the leukocyte to the endothelium, which can then initiate leukocyte interaction with the endothelium.[15,43] Blood flow velocity is largely dependent on pressure gradients and fluctuates over time within the same vessel due to spontaneous rhythmical contractions in the terminal arterioles.[21] Capillary pressure depends on the relative height of the capillary to the heart level and increases with temperature.[44] It can vary significantly among nearby similar-sized vessels. Hypertension does not significantly affect capillary pressure. Increased peripheral resistance in hypertension occurs at the precapillary level.[19,45] Due to these alterations, as well as different sampling depths of competing measurement techniques, there is a wide range of reported RBC velocities in human skin varying from 0 to 900 μm/sec.[21,46,47]

Under physiologic conditions, leukocytes are the only blood cells that interact with an intact endothelium[48,49] to eventually migrate to the extravascular tissue. During inflammation, increased expression of specialized endothelial proteins causes leukocytes to roll, adhere and eventually extravasate into the tissue at a higher rate than in normal conditions.[50,51] The ability of leukocyte-endothelial interactions to track inflammation has been well characterized in mouse models by *in vivo* labeled-cell[52–54] or label-free[55] intravital microscopy either noninvasively in the ear skin[56] or retina,[57,58] or invasively in exteriorized venules.[59,60] The number of rolling, adherent and extravasated leukocytes and the blood flow velocity are significantly altered during inflammation.[61,62] In humans, however, the noninvasive study of individual leukocyte behavior has been limited to the eye[63] and sublingual mucosa.[64]

In this study, we characterized individual cell motion in the upper dermal microvasculature of healthy human skin by noninvasive reflectance confocal video microscopy. In addition to visualizing previously described adherent and rolling leukocytes, we visualized temporary stopping of leukocytes ("paused" leukocytes)[20] in human skin microvasculature, which has been previously described in a broad range of animal species (also referred to as plugging,[20,22,31–35,23–30] stopping,[28,30,34,36,37] trapping[21,23–25,28,30,31,34,35] or retaining[22,25,28,31,34,35,37] of leukocytes). This work provides new insights into cell dynamics in intact human skin blood vessels. Through the detailed data acquisition protocol and method to extract quantitative parameters from reflectance confocal videos, this study will enable further exploration of the diagnostic potential for various clinical applications.

MATERIALS & METHODS

Reflectance Confocal Video Microscopy

We used a commercial reflectance confocal microscope, the VivaScope 1500 (Caliber I.D., Rochester NY), which is FDA-approved for clinical use in routine patient care. It illuminates the tissue with a near-infrared (830 nm) low-power (<20 mW) diode laser. Through a pinhole, the reflected light from a selected depth up to 200 μm deep in the tissue is collected at the detector. By stepwise movement of the object table, a 0.5×0.5 mm^2 image with 0.7–0.9 μm lateral and ~2–5 μm axial resolution[65] is formed at 9 frames per second. Mosaicking enables acquiring a total field of view (FOV) of 8×8 mm^2. The contrast in RCM images is achieved due to light that is backscattered as a result of variations in refractive indices of different skin structures.

Study Participants

Throughout 2018, we enrolled ten healthy subjects (5 male, 5 female) aged 18–76. Nine had Fitzpatrick skin type I-III, whereas one had type V. We excluded subjects with any type of autoimmune disease or any visible rash on the day of imaging (e.g. a scratch or a sunburn). All subjects reported feeling well and generally healthy on the day of the imaging. The study was approved by the Vanderbilt Institutional Review Board. All subjects gave informed consent.

Data Acquisition Protocol

Each subject was seated in a comfortable position 10 minutes prior to the procedure in a temperature-controlled room (22±1°C). We imaged left volar forearm and left upper anterior chest. During imaging, the subject's forearm rested on a pillow in a supine position parallel to the floor, ~10–20 cm below the heart level. During imaging of the chest, the subject lay supine, with back parallel to the ground or elevated as much as 30° for patient comfort. The measurement took 30–45 minutes per body site, 90–120 minutes in total. The data acquisition protocol is shown in Table 2.

UVB Light-Induced Inflammation

In one healthy subject (Fitzpatrick skin type II), we irradiated the left anterior thigh skin with 120 mJ UVB light for 75 seconds to cause an inflammatory reaction. We chose a dose slightly lower than that of standard initial psoriasis treatment for Fitzpatrick skin type I (130 mJ), and irradiated the skin for a much shorter time than a typical psoriasis treatment session (15–30 minutes).[66]

Image Registration

To remove motion artefacts due to breathing or movement, all images within the video were registered by using *Fiji* software[67] plugin *Linear Stack Alignment with SIFT*[68] with the following parameters: pixel initial gaussian blur of 1.6, feature descriptor size of 4, feature descriptor orientation bins of 8, maximal alignment error of 1 pixel, inlier ratio of 0.05, and affine transformation.

Estimation of Quantitative Parameters Characteristic of Skin Microcirculation

Table 3 defines 9 quantitative parameters characteristic of the upper dermal microvasculature of human skin.

Density of cutaneous blood vessels—We counted the number of vessels with clearly visible blood flow per video with a 0.5×0.5 mm^2 FOV. The mean of 10 videos (10 different 0.5×0.5 mm^2 FOVs) per body site was used for further statistical analysis.

Flow width and interconnective tissue width—To estimate cutaneous blood vessel size, we measured two parameters: (1) flow width, and (2) interconnective tissue width. Each parameter was measured at three different locations of the blood vessel within the same FOV to account for variation in its size. The mean of three measurements per vessel was then used to calculate the mean of 5 vessels per body site before further statistical analysis.

Flowing leukocyte velocity—We calculated the velocity of freely flowing leukocytes or leukocytes that do not appear to be squeezing through a narrow vessel or interacting with the endothelium. In *en face* RCM videos, we typically observed a portion of the vessel ~50–200 μm in length that is parallel to the skin surface. This enabled tracking a single flowing leukocyte in 2 to 5 consecutive frames. We used a *Fiji* software[67] plugin *Manual Tracking* to automatically calculate the velocity between each two consecutive frames (0.11 seconds between frames) after manually marking the center of a leukocyte in each frame. We determined the mean velocity and standard deviation of each flowing leukocyte. We tracked 5 different leukocytes within the same vessel at different time points throughout the 30-second video, and repeated it in 5 different vessels, resulting in the velocity measurements of 25 freely flowing leukocytes per imaging site, 50 in total per subject. Mean and/or median velocity was then calculated (1) per vessel by using the mean single leukocyte velocities; (2) per body site in a single subject by using the mean vessel velocities; (3) per body site in all 10 subjects by using a) the mean velocities per each subject and alternatively b) the mean velocities of all measured leukocytes.

Number of adherent, rolling and paused leukocytes—We counted all paused and all adherent leukocytes and measured their size. We determined the elapsed time between the paused leukocyte stopping and continue moving. Additionally, we searched for rolling leukocytes or leukocytes that appear to be moving forward in a rotational motion along the vessel wall.

Leukocyte size—We measured the width of each paused and adherent leukocyte on three different axes to account for variation in leukocyte shape. The mean of the three measured values was used for further statistical analysis.

Statistical Analysis

Median and interquartile range (IQR) of each parameter was calculated per 10 healthy subjects. Pearson's correlation coefficient was used to determine the correlation between (1) the time of leukocyte being paused and leukocyte or blood vessel size, and (2) the flowing

leukocyte velocity and flow or interconnective tissue width. All measurements and analyses were done by IS.

RESULTS

Description of Human Microvasculature in terms of (i) Density and (ii) Size of Cutaneous Blood Vessels, (iii) Leukocyte Velocity, and (iv) Leukocyte Interaction with the Endothelium

Reflectance confocal microscopy (RCM) videos enable the visualization of the motion of cells within the dermal papillae of intact human skin (Figure 1). We observed leukocytes as bright individual cells ~4–13 μm in width. A stationary leukocyte is usually round in shape, whereas a flowing leukocyte in a narrow, single-cell blood vessel is either round or elliptical in shape. We generally could not distinguish individual RBCs or individual platelets and visualized them as a mass of mildly reflective moving structures.

Once attached to the skin, the Vivascope 1500 enables video acquisition of a 0.5×0.5 mm^2 *en face* view of the skin within an 8×8 mm^2 total FOV at 9 frames per second. In each healthy subject, we acquired ten 30-second videos of the upper dermal microvasculature per body site: (1) left volar forearm, and (2) left upper anterior chest. This resulted in 10 videos or 5 minutes of videos per body site, 20 videos or 10 minutes of videos per subject.

Density of Cutaneous Blood Vessels.—We imaged 12 to 33 blood vessels per 10 videos (5 minutes total) per subject in the forearm (median amongst 10 subjects: 21), and 14 to 38 blood vessels per 10 videos in the chest (median: 18). The average density was 2 upper dermal blood vessels per 0.5×0.5 mm^2 FOV in both sites.

Blood Vessel Size.—Between the flow of cells and the surrounding connective tissue, we observed a hyporeflective band along each side of the flow (Figure 2). Blood vessel walls are not clearly visible by RCM. Therefore, we can only obtain bounding estimates of the true vessel width. We assumed that a blood vessel is not smaller than the width of cells flowing within the blood vessel and correspondingly measured flow width (w_{flow}) as the lower bound of the width (Figure 2 a,d). Assuming that blood vessel walls do not extend into the surrounding connective tissue, we measured interconnective tissue width (w_{tissue}) as the upper bound (Figure 2 a,d). We cannot be certain whether an adherent leukocyte is inside or outside the blood vessel (Figure 2). The average blood vessel flow width per each of the 10 healthy subjects ranged from 4 to 7 μm, whereas the interconnective tissue width ranged from 10 to 19 μm (Figure 3a). We imaged similar-sized vessels in both body sites, with a median flow width of 5 μm (both chest and forearm) and a median interconnective tissue width of 16 μm (forearm) and 14 μm (chest). We found no correlation (R^2=0.3) between the flow width and the interconnective tissue width (Figure 3b). The width of the hyporeflective band along each side of the flow ($\frac{1}{2}[w_{tissue} - w_{flow}]$) ranged from 1 to 11 μm (median: 4 μm) for all measured blood vessels.

Flowing Leukocyte Velocity Obeys Lognormal Distribution and Has No Correlation with Flow Width or Interconnective Tissue Width

In each vessel, we observed each single freely flowing leukocyte in as many consecutive frames as possible (typically 2 to 5). Flowing leukocyte velocities could have a very large range in a single vessel over the course of 30 seconds (e.g. 70–300 μm/sec for subject 5 chest vessel 2 shown in Figure 4a). The velocity range of leukocytes across multiple vessels was not significantly greater (e.g. 40–430 μm/sec in the chest and 10–240 μm/sec in the forearm of subject 5 shown in Figure 4b). All flowing leukocyte velocities per each site in a single subject followed a log-normal distribution with a higher velocity in the chest (median for subject 5 shown in Figure 4c: 143 μm/sec) than in the forearm (47 μm/sec). Although we found a large velocity variation within single and among nearby vessels in each subject, when the entire set of leukocyte velocities from the 10 subject study population was analyzed (Figure 4d, 4e, and 4f), most leukocytes had velocities ranging from 52–131 μm/sec (interquartile range from Figure 4f) and were log-normally distributed (Figure 4f). The average flowing leukocyte velocity taken per each of the 10 subjects (Figure 4e) was typically two times higher in the chest (median across all subjects 117 μm/sec) than in the forearm (66 μm/sec). We found no correlation (R^2<0.01) between the flowing leukocyte velocity and flow or interconnective tissue width.

We Found No Rolling and a Few Adherent Leukocytes in the Upper Dermal Blood Vessels of Healthy Forearm and Upper Chest Skin

Leukocyte adhesion and rolling is significantly increased during inflammation.[69] Per our definition of a leukocyte stationary next to the vessel wall that does not move for at least 30 seconds and does not stop the rest of the blood flow (Table 3), we observed at least one adherent leukocyte[70] (Figure 2a–c) in the forearm of 6 and in the chest of 4 out of 10 healthy subjects. We found a median of 2 adherent leukocytes in the forearm and 0 in the chest per 10 videos, 5 minutes of videos per subject (Figure 3a). In healthy-appearing forearm skin of a 73-year-old female who reported no health issues, we found 13 adherent leukocytes, an outlier in our data. We found no rolling leukocytes in any of the 10 subjects.

Upper Dermal Blood Vessels Have “Paused” Leukocytes that Temporarily Stop, Coinciding with the Stopping of the Blood Flow

Whereas adherent leukocytes are paused next to the blood vessel wall for at least 30 seconds while the rest of the blood cells continue to flow (Figure 2a–c), we also observed leukocytes that appear to freely move with the rest of the flow until temporarily stopping, coinciding with the simultaneous stopping of the rest of the blood flow (Figure 2d–f). We term these “paused” leukocytes. We observed paused leukocytes in the forearm of 7 and in the chest of 5 subjects. We found a median of 1 paused leukocyte in the forearm and 0 in the chest per 10 videos, 5 minutes of videos per subject (Figure 3c). In contrast to adherent leukocytes, paused leukocytes resumed their motion during the 30 second video, along with resumption of flow of the rest of the blood in the vessel. Paused leukocytes were located *within* the flow space (Figure 2d–f). By contrast, adherent leukocytes were located *outside* of the flow space, but within the interconnective tissue space (Figure 2a–c). Freely flowing, paused and adherent leukocytes appeared similar in size with a median of 6 to 8 μm (Figure 3d–e).

Paused leukocytes (n=24) stopped for 1–29 seconds for a median of 7 seconds in the forearm and 3 seconds in the chest (Figure 3f). We found no correlation (R^2<0.5) between the time of a leukocyte being paused and any parameter characteristic of blood vessel or leukocyte size. Overall, we observed almost 4 times more adherent and paused leukocytes in the forearm (n=40) than in the chest (n=12).

Leukocytes Roll After Induced Inflammation in Healthy Skin

To test whether inflammation causes leukocyte rolling in the topmost blood vessels of healthy skin, we imaged the left anterior thigh of one healthy volunteer (Fitzpatrick skin type II) before and 30 minutes after irradiation with 120 mJ UVB light for 75 seconds, which caused a heating sensation in the irradiated ~5–10 cm^2 skin area. We tried to image the same exact 8×8 mm^2 FOV by marking the skin with a surgical pen. We saw no rolling leukocytes in the baseline measurement but visualized several rolling leukocytes in one blood vessel 30 minutes post UVB light-induced inflammation (video available in supplementary material S4). We saw no adherent leukocyte before or after UVB light irradiation.

Blood Flow in the Upper Dermal Vessels Changes Direction

We observed the blood flow change direction in four 30-second videos of three subjects: in the forearm of a 76-year-old female and a 68-year-old male, and in the forearm and chest of a 70-year-old male (video available in supplementary material S5).

DISCUSSION

In this study, we described the upper dermal microvasculature of healthy human skin through nine quantitative parameters and reported the range of these parameter values in ten healthy subjects. In addition to visualizing previously described adherent and rolling leukocytes, we visualized temporary stopping of leukocytes ("paused" leukocytes)[20] in human skin microvasculature, which has been previously described in a broad range of animal species (also referred to as plugging,[20,22,31–35,23–30] stopping,[28,30,34,36,37] trapping,[21,23–25,28,30,31,34,35] or retaining[22,25,28,31,34,35,37] of leukocytes). We found no rolling leukocytes in healthy skin under normal conditions. In one healthy volunteer, we visualized several rolling leukocytes 30 minutes after UVB light irradiation. Flowing leukocyte velocities followed a log-normal distribution with the median velocity higher in upper chest (117 μm/sec) than volar forearm (66 μm/sec). We observed blood flow change direction.

We visualized, on average, two upper dermal blood vessels per 0.5×0.5 mm^2 *en face* FOV, resulting in around 40 analyzed vessels per subject. Because the coordinated recruitment of leukocytes is largely confined to postcapillary venules,[71] we hypothesize that we visualized both *capillaries* (narrow, single-cell vessels) and *postcapillary venules*. Consistent with an earlier study by Rajadhyaksha et. al.,[72] we observed leukocytes distending the flow width during their passage, but our measured flow width values (4–7 μm) were slightly lower than these previous findings (8±2 μm).[72] We frequently observed adherent leukocytes outside of the flow width, therefore we introduced interconnective tissue width as an additional parameter inclusive of an ~4 μm wide hyporeflective band observed along each side of the

flow (Figure 2). We hypothesize that we visualized adherent leukocytes *within* a postcapillary venule and that the true diameter of these particular vessels is more likely represented by the interconnective tissue width (10–19 μm) than the flow width (4–7 μm). We speculate that the ~1–11 μm (median: 4 μm) hyporeflective, dark band along each side of the flow is endothelial glycocalyx, a layer of glycoproteins and glycolipids.[73] Consistent with our observations (Figure 2), glycocalyx is free of red blood cells and platelets, whereas leukocytes traverse it to interact with the endothelium.[73] Although small animal studies report glycocalyx as <0.5 μm thick in capillaries (~10–15% of diameter),[73–75] it has been reported 1 μm thick in human sublingual and 9 μm in human retinal capillaries.[76] Interestingly, our measured flow width values (4–7 μm) matched the internal (4–6 μm) *capillary* diameter values reported in an *ex vivo* study of human forearm skin capillary.[10] Our interconnective tissue width values (10–19 μm), however, were generally larger than the reported external (8–12 μm)[10,11] *capillary* diameter values, but matched the internal (10–15 μm)[6] and external (18–23 μm)[6] diameter values of *postcapillary venules*.

We visualized individual freely flowing, paused and adherent leukocytes in healthy skin under normal conditions, and rolling leukocytes 30 minutes after UVB light irradiation. Takeishi et. al. showed that in narrow, single-cell capillaries, transforming to an elliptical shape enables leukocytes to firmly adhere to the vessel wall.[77] Interestingly, we frequently observed ellipse-shaped leukocytes freely flow and pause with the rest of the blood flow, whereas adherent and rolling leukocytes were always round in shape. Moreover, paused leukocytes were always measured within the flow width, whereas adherent and rolling leukocytes were typically outside of the flow width but within the interconnective tissue width. Normal blood flow was commonly visible within the flow width immediately adjacent to the adherent and rolling leukocytes (supplementary materials S2 an S5). Pixel brightness within an adherent leukocyte fluctuated over time, making it appear active, although not moving in any direction. Adherent leukocytes eventually extravasate through the blood vessel walls into the surrounding tissue.[78,79] Although we did not observe the process of extravasation in any subject, it has been observed in human skin by RCM (personal communication with Christi Fox, Caliber I.D.). RCM enables visualization of blood cell motion in the topmost capillaries of any Fitzpatrick skin type.

We characterized individual leukocyte motion based on the number of adherent, rolling and paused leukocytes, the time of leukocyte being paused, and the flowing leukocyte velocity. We observed leukocytes as bright, reflective round to oval cells 4–13 μm in size. Some visualized smaller cells <8 μm in width could be RBCs, although we generally did not clearly distinguish individual RBCs or platelets. Moreover, RBCs tend to change their shape in single-cell vessels,[18] likely appearing smaller than their largest dimension. We visualized paused leukocytes that temporarily stopped for 1–29 seconds, coinciding with the simultaneous stopping of the rest of the blood flow. Interestingly, we found no correlation between the time of leukocyte pause and leukocyte or blood vessel size. We also found no correlation between the flowing leukocyte velocity and the flow or interconnective tissue width. We observed blood flow change direction in four 30-second videos of three of our four subjects above 50 years old. This may indicate change in afferent or efferent blood vessel pressure, and further studies are needed to evaluate the correlation between this observation and subject age.

A fundamental limitation of this technique is the decreasing spatial resolution with an increase in imaging depth. Because of spherical aberration effects, as well as light scattering due to different refractive indices of the epidermis and dermis, the experimentally observed spatial resolution (~0.7–0.9 μm) in the upper dermis is lower than the theoretical limit (~0.5 μm).[65,80] Thus, we typically observed the flow or interaction with the endothelium of individual cells only up to ~60–80 μm deep in the tissue. In addition to measuring leukocyte size within the imaging plane (two-dimensional image), its size could additionally be measured across the z axis (depth) for a more accurate estimation. Although our protocol involved measuring 10 different 0.5×0.5 mm^2 areas within 8×8 mm^2 per body site, the measured parameter values depend on selected imaging area and depth. In addition to density of blood vessels, the area filled with blood vessels could be measured.[81,82] The presented method and results of this study will aid future clinical studies to assess the diagnostic potential of parameters characteristic of individual blood vessels and individual cell motion.

PERSPECTIVES

We present the characteristics of *in vivo* leukocyte-endothelial interactions and intact human skin microvasculature, including the presence of paused, adherent and rolling leukocytes. This opens a new avenue for studying skin microvasculature at the individual cell level with an emerging clinical modality, reflectance confocal video microscopy. The described method and range of values in healthy skin will enable future studies to evaluate the diagnostic potential of these parameters in cardiovascular, inflammatory and immune diseases.

Supplementary Material

Refer to Web version on PubMed Central for supplementary material.

ACKNOWLEDGMENTS

We are grateful to all volunteers who participated in this study. The work was supported by the Vanderbilt University Medical Center Departments of Medicine, Career Development Award Number IK2 CX001785 from the United States Department of Veterans Affairs Clinical Sciences R&D (CSRD) Service, and the National Institutes of Health Grant K12 CA090625. We thank Milind Rajadhyaksha, Aditi Sahu and Kivanc Kose of Memorial Sloan Kettering Cancer Center for many helpful conversations in preparing this manuscript.

LIST OF ABBREVIATIONS

RCM	reflectance confocal microscopy
DEJ	dermal-epidermal junction
RBC	red blood cell
FOV	field of view
IQR	interquartile range
FDA	Food and Drug Administration
UVB	Type B ultraviolet light

REFERENCES

1. Da Luz PL, Libby P, Laurindo FRM, Chagas ACP. Endothelium and Cardiovascular Diseases: Vascular Biology and Clinical Syndromes. Academic Press; 2018.
2. Lancaster G, Stefanovska A, Pesce M, et al. Dynamic markers based on blood perfusion fluctuations for selecting skin melanocytic lesions for biopsy. Sci Rep. 2015;5:1–13. doi:10.1038/srep12825
3. Östlund Papadogeorgos N, Jörneskog G, Bengtsson M, Kahan T, Kalani M. Severely impaired microvascular reactivity in diabetic patients with an acute coronary syndrome. Cardiovasc Diabetol. 2016;15(1):1–6. doi:10.1186/s12933-016-0385-6 [PubMed: 26739706]
4. Alba BK, Greaney JL, Ferguson SB, Alexander LM. Endothelial function is impaired in the cutaneous microcirculation of adults with psoriasis through reductions in nitric oxide-dependent vasodilation. Am J Physiol Circ Physiol. 2017;314(2):H343–H349. doi:10.1152/ajpheart.00446.2017
5. Lal C, Leahy MJ. An Updated Review of Methods and Advancements in Microvascular Blood Flow Imaging. Microcirculation. 2016;23(5):345–363. doi:10.1111/micc.12284 [PubMed: 27096736]
6. Braverman IM. The cutaneous microcirculation: Ultrastructure and microanatomical organization. Microcirculation. 1997;4(3):329–340. doi:10.3109/10739689709146797 [PubMed: 9329009]
7. Braverman IM, Yen A. Ultrastructure of the human dermal microcirculation: II. The capillary loops of the dermal papillae. J Invest Dermatol. 1977;68(1):44–52. doi:10.1111/1523-1747.ep12485165 [PubMed: 830769]
8. Yen A, Braverman IM. Ultrastructure of the human dermal microcirculation: the horizontal plexus of the papillary dermis. J Invest Dermatol. 1976;66(3):131–142. doi:10.1111/1523-1747.ep12481678 [PubMed: 1249441]
9. Geyer SH, Nöhammer MM, Tinhofer IE, Weninger WJ. The dermal arteries of the human thumb pad. J Anat. 2013;223(6):603–609. doi:10.1111/joa.12113 [PubMed: 24205910]
10. Braverman IM. The cutaneous microcirculation. J Investig Dermatology Symp Proc. 2000;5(1):3–9. doi:10.1046/j.1087-0024.2000.00010.x
11. Archid R, Patzelt A, Lange-Asschenfeldt B, et al. Confocal laser-scanning microscopy of capillaries in normal and psoriatic skin. J Biomed Opt. 2012;17(10):101511. doi:10.1117/1.jbo.17.10.101511 [PubMed: 23223987]
12. Diez-Silva M, Dao M, Han J, Lim C-T, Suresh S. Shape and Biomechanical Characteristics of Human Red Blood Cells in Health and Disease. MRS Bull. 2010;35(5):382–388. doi:10.1557/mrs2010.571 [PubMed: 21151848]
13. Thon J, Italiano J. Platelet formation. Semin Hematol. 2010;47(3):220–226. doi:10.1053/j.seminhematol.2010.03.005.PLATELET [PubMed: 20620432]
14. Schmid-Schonbein GW, Shih YY, Chien S. Morphometry of human leukocytes. Blood. 1980;56(5):866–875. doi:10.1182/blood.v56.5.866.bloodjournal565866 [PubMed: 6775712]
15. Schmid-schonbein GW. Leukocyte kinetics in the microcirculation. Biorheology. 1987;24(2):139–151. [PubMed: 3651587]
16. Ting-Beall HP, Needham D, Hochmuth RM. Volume and osmotic properties of human neutrophils. Blood. 1993;81(10):2774–2780. doi:10.1182/blood.v81.10.2774.bloodjournal81102774 [PubMed: 8490184]
17. Shapiro HM, Schildkraut ER, Curbelo R, Laird CW, Turner RB, Hirschfeld T. Combined blood cell counting and classification with fluorochrome stains and flow instrumentation. J Histochem Cytochem. 1976;24(1):396–411. [PubMed: 56391]
18. Secomb TW. Blood Flow in the Microcirculation. Annu Rev Fluid Mech. 2016;49(1):443–461. doi:10.1146/annurev-fluid-010816-060302
19. Caro CG, Pedley TJ, Schroter RC, Seed WA. The Mechanics of the Circulation. Cambridge University Press; 2012.
20. Tam J, Tiruveedhula P, Roorda A. Characterization of single-file flow through human retinal parafoveal capillaries using an adaptive optics scanning laser ophthalmoscope. Biomed Opt Express. 2011;2(4):781. doi:10.1364/boe.2.000781 [PubMed: 21483603]

21. Hahn M, Klyscz T, Jünger M. Synchronous measurements of blood pressure and red blood cell velocity in capillaries of human skin. J Invest Dermatol. 1996;106(6):1256–1259. doi:10.1111/1523-1747.ep12348955 [PubMed: 8752666]
22. Hokama JY, Ritter LS, Davis-Gorman G, Cimetta AD, Copeland JG, McDonagh PF. Diabetes enhances leukocyte accumulation in the coronary microcirculation early in reperfusion following ischemia. J Diabetes Complications. 2000;14(2):96–107. doi:10.1016/S1056-8727(00)00068-4 [PubMed: 10959072]
23. Engler RL, SchmidSchonbein GW, Pavelec RS. Leukocyte capillary plugging in myocardial ischemia and reperfusion in the dog. Am J Pathol. 1983;111(1):98–111. [PubMed: 6837725]
24. Eppihimer MJ, Lipowsky HH. Leukocyte sequestration in the microvasculature in normal and low flow states. Am J Physiol - Hear Circ Physiol. 1994;267(3 36–3). doi:10.1152/ajpheart.1994.267.3.h1122
25. Eppihimer MJ, Lipowsky HH. Effects of leukocyte-capillary plugging on the resistance to flow in the microvasculature of cremaster muscle for normal and activated leukocytes. Microvasc Res. 1996;51(2):187–201. doi:10.1006/mvre.1996.0020 [PubMed: 8778574]
26. Harris AG, Skalak TC, Hatchell DL. Leukocyte-capillary plugging and network resistance are increased in skeletal muscle of rats with streptozotocin- induced hyperglycemia. Int J Microcirc Exp. 1994;14(3):159–166. doi:10.1159/000178824
27. Miyamoto K, Hiroshiba N, Tsujikawa A, Ogure Y. In Vivo Demonstration of Increased Leukocyte Entrapment in Retinal Microcirculation of Diabetic Rats. Investig Ophthalmol Vis Sci. 1998;39(11):2190–2194. [PubMed: 9761301]
28. Ritter LS, Wilson DS, Williaiis SK, Copeland JG, Mcdonagh PF. Early in reperfusion following myocardial ischemia, leukocyte activation is necessary for venular adhesion but not capillary retention. Microcirculation. 1995;2(4):315–327. [PubMed: 8714813]
29. Yang Y Visualization of retinal and choroidal blood flow with fluorescein leukocyte angiography in rabbits. Graefe's Arch Clin Exp Ophthalmol. 1997;235(1):27–31. doi:10.1007/BF01007834 [PubMed: 9034839]
30. Nishiwaki H, Ogura Y. Evaluation of leukocyee dynamics in retinal microcirculation. Japanese J Clin Ophthalmol. 1995;49(8):1393–1397.
31. Schroder S, Palinski W, Schmid-Schonbein GW. Activated monocytes and granulocytes, capillary nonperfusion, and neovascularization in diabetic retinopathy. Am J Pathol. 1991;139(1):81–100. [PubMed: 1713023]
32. Mehta JL, Nichols WW, Schofield R, Donnelly WH, Chandna VK. TxA2 inhibition and ischemia-induced loss of myocardial function and reactive hyperemia. Am J Physiol - Hear Circ Physiol. 1990;258(5 27–5). doi:10.1152/ajpheart.1990.258.5.h1402
33. Harris AG, Steinbauer M, Leiderer R, Messmer K. Role of leukocyte plugging and edema in skeletal muscle ischemia- reperfusion injury. Am J Physiol - Hear Circ Physiol. 1997;273(2 42–2):989–996. doi:10.1152/ajpheart.1997.273.2.h989
34. Ritter LS, Mcdonagh PF. Low-flow reperfusion after myocardial ischemia enhances leukocyte accumulation in coronary microcirculation. Am J Physiol - Hear Circ Physiol. 1997;273(3 42–3). doi:10.1152/ajpheart.1997.273.3.h1154
35. Ritter LS, Copeland JG, McDonagh PF. Fucoidin reduces coronary microvascular leukocyte accumulation early in reperfusion. Ann Thorac Surg. 1998;66(6):2063–2071. doi:10.1016/S0003-4975(98)00823-6 [PubMed: 9930494]
36. Takasu I, Shiraga F, Okanouchi T, Tsuchida Y, Ohtsuki H. Evaluation of leukocyte dynamics in choroidal circulation with indocyanine green-stained leukocytes. Investig Ophthalmol Vis Sci. 2000;41(10):2844–2848. [PubMed: 10967036]
37. Fillacier K, Peyman GA, Luo Q, Khoobehi B. Study of lymphocyte dynamics in the ocular circulation: Technique of labeling cells. Curr Eye Res. 1995;14(7):579–584. doi:10.3109/02713689508998405 [PubMed: 7587304]
38. Kuebler WM, Kuhnle GEH, Groh J, Goetz AE. Leukocyte kinetics in pulmonary microcirculation: Intravital fluorescence microscopic study. J Appl Physiol. 1994;76(1):65–71. doi:10.1152/jappl.1994.76.1.65 [PubMed: 8175549]

39. Bollinger A, Butti P, Barras JP, Trachsler H, Siegenthaler W. Red blood cell velocity in nailfold capillaries of man measured by a television microscopy technique. Microvasc Res. 1974;7(1):61–72. doi:10.1016/0026-2862(74)90037-5 [PubMed: 4206888]
40. Schmid-Schoenbein GW, Zweifach BW. RBC velocity profiles in arterioles and venules of the rabbit omentum. Microvasc Res. 1975;10(2):153–164. doi:10.1016/0026-2862(75)90003-5 [PubMed: 1186523]
41. Sun C, Migliorini C, Munn LL. Red blood cells initiate leukocyte rolling in postcapillary expansions: A lattice Boltzmann analysis. Biophys J. 2003;85(1):208–222. doi:10.1016/S0006-3495(03)74467-1 [PubMed: 12829477]
42. Lowe GDO. Clinical Blood Rheology. Vol 2 Crc Press; 2019.
43. Schmid-Schönbein GW, Usami S, Skalak R, Chien S. The interaction of leukocytes and erythrocytes in capillary and postcapillary vessels. Microvasc Res. 1980;19(1):45–70. doi:10.1016/0026-2862(80)90083-7 [PubMed: 7360047]
44. Landis EM. Micro-injection studies of capillary blood pressure in human skin. Heart. 1930;15:209–228.
45. Eichna LW, Bordley J. Capillary Blood Pressure in Man. Comparison of Direct and Indirect Methods of Measurement. 1. J Clin Invest. 2008;18(6):695–704. doi:10.1172/jci101085
46. Fagrell B, Fronek A, Intaglietta M. A microscope-television system for studying flow velocity in human skin capillaries. Am J Physiol. 1977;233(2):H318–21. [PubMed: 888975]
47. Stücker M, Baier V, Reuther T, Hoffmann K, Kellam K, Altmeyer P. Capillary blood cell velocity in human skin capillaries located perpendicularly to the skin surface: Measured by a new laser Doppler anemometer. Microvasc Res. 1996;52(2):188–192. doi:10.1006/mvre.1996.0054 [PubMed: 8901447]
48. Rumbaut RE, Thiagarajan P. Platelet-vessel wall interactions in hemostasis and thrombosis. Synth Lect Integr Syst Physiol From Mol to Funct. 2010;2(1):1–75.
49. Oberleithner H, Wälte M, Kusche-Vihrog K. Sodium renders endothelial cells sticky for red blood cells. Front Physiol. 2015;6(JUN):2011–2016. doi:10.3389/fphys.2015.00188
50. Huzaira M, Gonzalez S. Graft-versus-host disease, as seen by reflectance confocal microscopy and correlation with the corresponding histology. J Invest Dermatol. 2003;121(1):0374.
51. Mempel TR, Scimone ML, Mora JR, Von Andrian UH. In vivo imaging of leukocyte trafficking in blood vessels and tissues. Curr Opin Immunol. 2004;16(4):406–417. doi:10.1016/j.coi.2004.05.018 [PubMed: 15245733]
52. Ley K, Kansas GS. Selectins in T-cell recruitment to non-lymphoid tissues and sites of inflammation. Nat Rev Immunol. 2004;4(5):325–336. doi:10.1038/nri1351 [PubMed: 15122198]
53. Wang X, Fujita M, Prado R, et al. Visualizing CD4 T-cell migration into inflamed skin and its inhibition by CCR4/CCR10 blockades using in vivo imaging model. Br J Dermatol. 2010;162(3):487–496. doi:10.1111/j.1365-2133.2009.09552.x [PubMed: 19832835]
54. Germain RN, Miller MJ, Dustin ML, Nussenzweig MC. Dynamic imaging of the immune system: progress, pitfalls and promise. Nat Rev Immunol. 2006;6(7):497–507. doi:10.1038/nri1884 [PubMed: 16799470]
55. Tsai C-K, Chen Y-S, Wu P-C, et al. Imaging granularity of leukocytes with third harmonic generation microscopy. Biomed Opt Express. 2012;3(9). doi:10.1038/srep37210
56. Li JL, Goh CC, Keeble JL, et al. Intravital multiphoton imaging of immune responses in the mouse ear skin. Nat Protoc. 2012;7(2):221–234. doi:10.1038/nprot.2011.438 [PubMed: 22240584]
57. Parnaby-Price A, Stanford MR, Biggerstaff J, et al. Leukocyte trafficking in experimental autoimmune uveitis in vivo Abstract : Leukocyte trafficking from blood into tissue is a fundamental process in immune surveil- mental autoimmune uveitis (EAU) is an animal lymphocytes and macrophages that infiltrate. 1998;64(4):434–440.
58. Villani E, Baudouin C, Efron N, et al. In vivo confocal microscopy of the ocular surface: from bench to bedside. Curr Eye Res. 2014;39(3):213–231. doi:10.3109/02713683.2013.842592 [PubMed: 24215436]
59. Jung U, Bullard DC, Tedder TF, Ley K. Velocity differences between L- and P-selectin-dependent neutrophil rolling in venules of mouse cremaster muscle in vivo. Am J Physiol. 1996;271(6 Pt 2):2740–2747.

60. Celi A, Merrill-Skoloff G, Gross P, et al. Thrombus formation: Direct real-time observation and digital analysis of thrombus assembly in a living mouse by confocal and widefield intravital microscopy. J Thromb Haemost. 2003;1(1):60–68. doi:10.1046/j.1538-7836.2003.t01-1-00033.x [PubMed: 12871540]
61. Janssen GH, Tangelder GJ, Oude Egbrink MG, Reneman RS. Spontaneous leukocyte rolling in venules in untraumatized skin of conscious and anesthetized animals. Am J Physiol. 1994;267(3 Pt 2):H1199–204. [PubMed: 8092286]
62. Asaduzzaman M, Mihaescu A, Wang Y, Sato T, Thorlacius H. P-selectin and P-selectin glycoprotein ligand 1 mediate rolling of activated CD8+ T cells in inflamed colonic venules. J Investig Med. 2009;57(7):765–768. doi:10.231/JIM.0b013e3181b918fb
63. Kirveskari J, Vesaluoma MH, Moilanen JAO, et al. A novel non-invasive, in vivo technique for the quantification of leukocyte rolling and extravasation at sites of inflammation in human patients. Nat Med. 2001;7(3):376–379. doi:10.1038/85538 [PubMed: 11231641]
64. Fabian-Jessing BK, Massey MJ, Filbin MR, et al. In vivo quantification of rolling and adhered leukocytes in human sepsis. Crit Care. 2018;22(1):1–7. doi:10.1186/s13054-018-2173-z [PubMed: 29301549]
65. Dwyer PJ, Di Marzio CA, Rajadhyaksha M. Confocal theta line-scanning microscope for imaging human tissues. Appl Opt. 2007;46(10):1843–1851. doi:10.1364/AO.46.001843 [PubMed: 17356629]
66. Singh RK, Lee KM, Jose MV., et al. The Patient's Guide to Psoriasis Treatment. Part 1: UVB Phototherapy. Dermatol Ther (Heidelb). 2016;6(3):307–313. doi:10.1007/s13555-016-0129-2 [PubMed: 27474029]
67. Schindelin J, Arganda-Carreras I, Frise E, et al. Fiji: An open-source platform for biological-image analysis. Nat Methods. 2012;9(7):676–682. doi:10.1038/nmeth.2019 [PubMed: 22743772]
68. Lowe DG. Distinctive Image Features from Scale-Invariant Keypoints. Int J Comput Vis. 2004:1–28. doi:10.1023/B:VISI.0000029664.99615.94
69. Ley K, Bullard DC, Arbonés ML, et al. Sequential contribution of L- and P-selectin to leukocyte rolling in vivo. J Exp Med. 1995;181(2):669–675. doi:10.1084/jem.181.2.669 [PubMed: 7530761]
70. Forbes TL, Harris KA, Jamieson WG, DeRose G, Carson M, Potter RF. Leukocyte activity and tissue injury following ischemia-reperfusion in skeletal muscle. Microvasc Res. 1996;51(3):275–287. doi:10.1006/mvre.1996.0027 [PubMed: 8992228]
71. Granger DN, Senchenkova E. Leukocyte-Endothelial Cell Adhesion In: Inflammation and the Microcirculation. San Rafael, CA: Morgan & Claypool Life Sciences; 2010 https://www.ncbi.nlm.nih.gov/books/NBK53380/.
72. Rajadhyaksha M, Grossman M, Esterowitz D, Webb RH, Anderson RR. In vivo confocal scanning laser microscopy of human skin: melanin provides strong contrast. J Invest Dermatol. 1995;104(6):946–952. [PubMed: 7769264]
73. Reitsma S, Slaaf DW, Vink H, Van Zandvoort MAMJ, Oude Egbrink MGA. The endothelial glycocalyx: Composition, functions, and visualization. Pflugers Arch Eur J Physiol. 2007;454(3):345–359. doi:10.1007/s00424-007-0212-8 [PubMed: 17256154]
74. Potter DR, Damiano ER. The hydrodynamically relevant endothelial cell glycocalyx observed in vivo is absent in vitro. Circ Res. 2008;102(7):770–776. doi:10.1161/CIRCRESAHA.107.160226 [PubMed: 18258858]
75. Ebong EE, Macaluso FP, Spray DC, Tarbell JM. Imaging the endothelial glycocalyx in vitro by rapid freezing/freeze substitution transmission electron microscopy. Arter Thromb Vasc Biol. 2011;31(8):1908–1915. doi:10.1038/jid.2014.371
76. Broekhuizen LN, Lemkes BA, Mooij HL, et al. Effect of sulodexide on endothelial glycocalyx and vascular permeability in patients with type 2 diabetes mellitus. Diabetologia. 2010;53(12):2646–2655. doi:10.1007/s00125-010-1910-x [PubMed: 20865240]
77. Takeishi N, Imai Y, Ishida S, Omori T, Kamm RD, Ishikawa T. Cell adhesion during bullet motion in capillaries. Am J Physiol - Hear Circ Physiol. 2016;311(2):H395–H403. doi:10.1152/ajpheart.00241.2016

78. Nieminen M, Henttinen T, Merinen M, et al. Vimentin function in lymphocyte adhesion and transcellular migration. Nat Cell Biol. 2006;8(2):156–162. doi:10.1038/ncb1355 [PubMed: 16429129]

79. Lorenzl S, Koedel U, Dirnagl U, Ruckdeschel G, Pfister HW. Imaging of leukocyte-endothelium interaction using in vivo confocal laser scanning microscopy during the early phase of experimental pneumococcal meningitis. J Infect Dis. 1993;168(4):927–933. [PubMed: 7690826]

80. Rajadhyaksha M, González S, Zavislan JM, Anderson RR, Webb RH. In vivo confocal scanning laser microscopy of human skin II: Advances in instrumentation and comparison with histology. J Invest Dermatol. 1999;113(3):293–303. doi:10.1046/j.1523-1747.1999.00690.x [PubMed: 10469324]

81. Meiburger KM, Chen Z, Sinz C, et al. Automatic skin lesion area determination of basal cell carcinoma using optical coherence tomography angiography and a skeletonization approach: Preliminary results. J Biophotonics. 2019;(May):1–11. doi:10.1002/jbio.201900131

82. Aguirre J, Schwarz M, Garzorz N, et al. Precision assessment of label-free psoriasis biomarkers with ultra-broadband optoacoustic mesoscopy. Nat Biomed Eng. 2017;1(5):1–8. doi:10.1038/s41551-017-0068

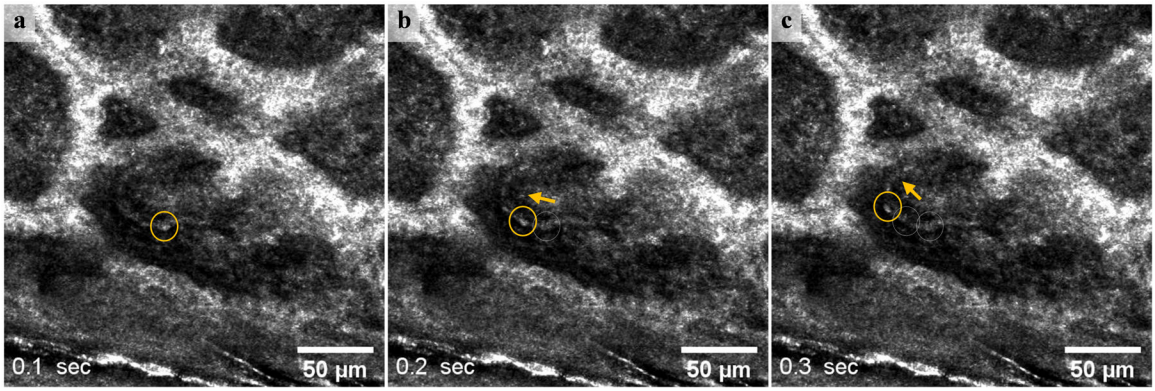

Figure 1.

A single blood cell 6±1µm in size (yellow circle) moving in a dermal blood vessel 60 µm below the skin surface at 0.1 second intervals (video available in supplementary material S1). The arrow shows the flow direction in the portion of the blood vessel that is parallel to the skin surface. Most blood cells appear as mildly reflective structures, with indistinguishable borders between them.

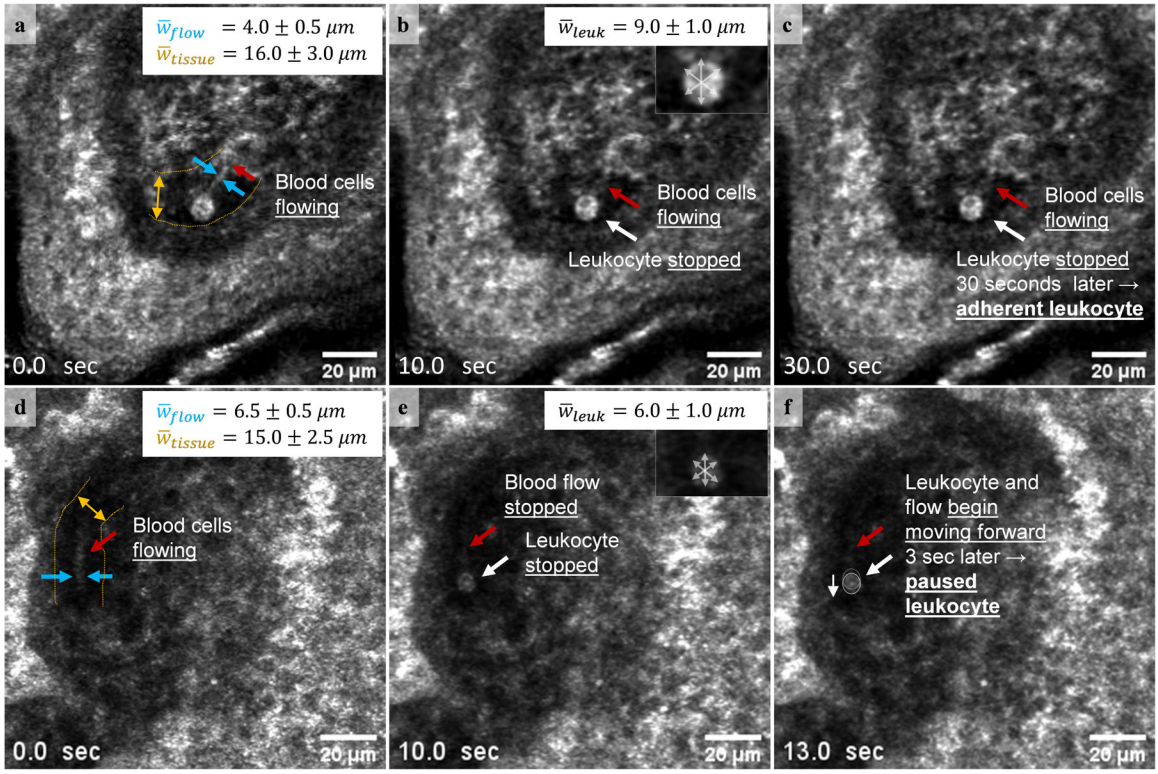

Figure 2.

A single measurement of flow width (blue arrows, **a** and **d**), interconnective tissue width (yellow arrow, **a** and **d**), and the average leukocyte size through measurements of 3 different axes (grey arrows, insets in **b** and **e**). **(a-c)** An adherent leukocyte (leukocyte stationary for at least 30 seconds) visualized next to moving blood cells (red arrow; video available in supplementary material S2) is 9.0±1.0 μm in width and within the interconnective tissue space (width 16.0±3.0 μm), but *outside the flow space* (width 4.0±0.5 μm). Note that we cannot be certain whether the adherent leukocyte is inside or outside the blood vessel. **(d-f)** In this example, a paused leukocyte (a leukocyte temporarily stopping, coinciding with the simultaneous stopping of the rest of the blood flow) and the blood flow stop for 3 seconds before resuming motion in the same direction (video available in supplementary material S3). Paused leukocyte 6.0±1.0 μm in width is *within the flow space* (width 6.5±0.5 μm) and within the interconnective tissue space (width 15.0±2.5 μm). Note that the adherent leukocyte appears larger and brighter than the paused leukocyte.

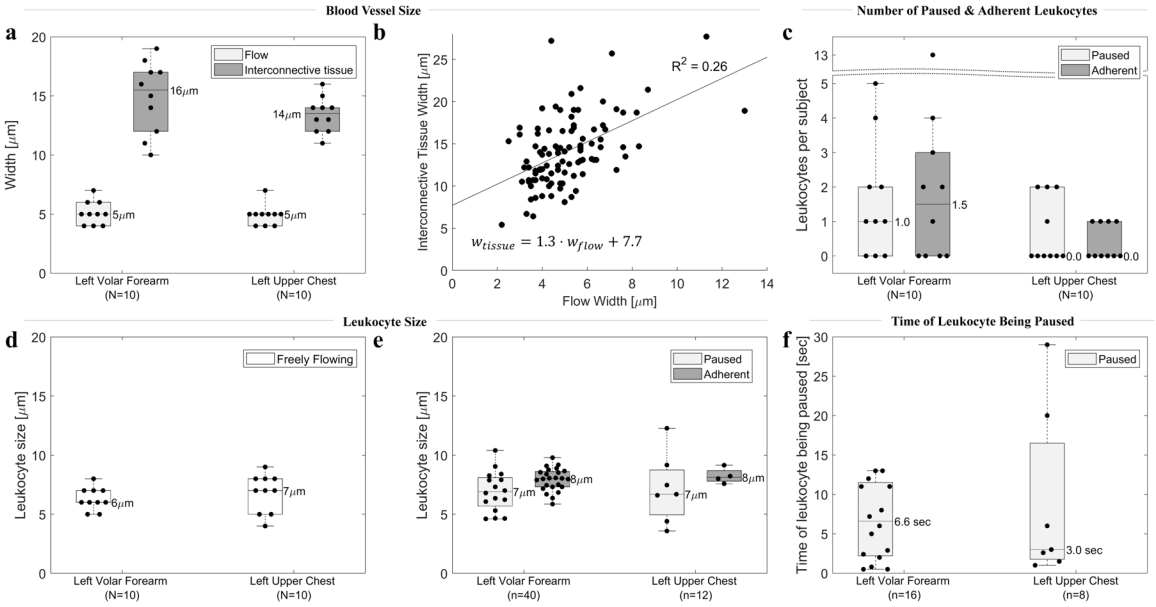

Figure 3.

Six quantitative parameters characteristic of blood vessel size and leukocyte-endothelial interactions in 10 healthy subjects, and their variation among two body sites. **(a)**. Upper (flow width) and lower (interconnective tissue width) bounds of blood vessel size. Each dot represents the average of 10 cutaneous blood vessels in each subject (N=10 subjects for 100 blood vessels total). **(b)** No correlation (R^2=0.26) between flow width and interconnective tissue width. **(c)** Number of paused and adherent leukocytes per 10 videos (5 minutes of video) per body site per subject. Each dot represents one subject (N=10). **(d,e)** Size of freely flowing, paused and adherent leukocytes. Each dot represents a single leukocyte. **(f)** Time of leukocyte being paused before resuming motion along with the rest of the flow. Each dot represents a single leukocyte. Note that in all graphs N represents the number of subjects, whereas n represents the number of leukocytes.

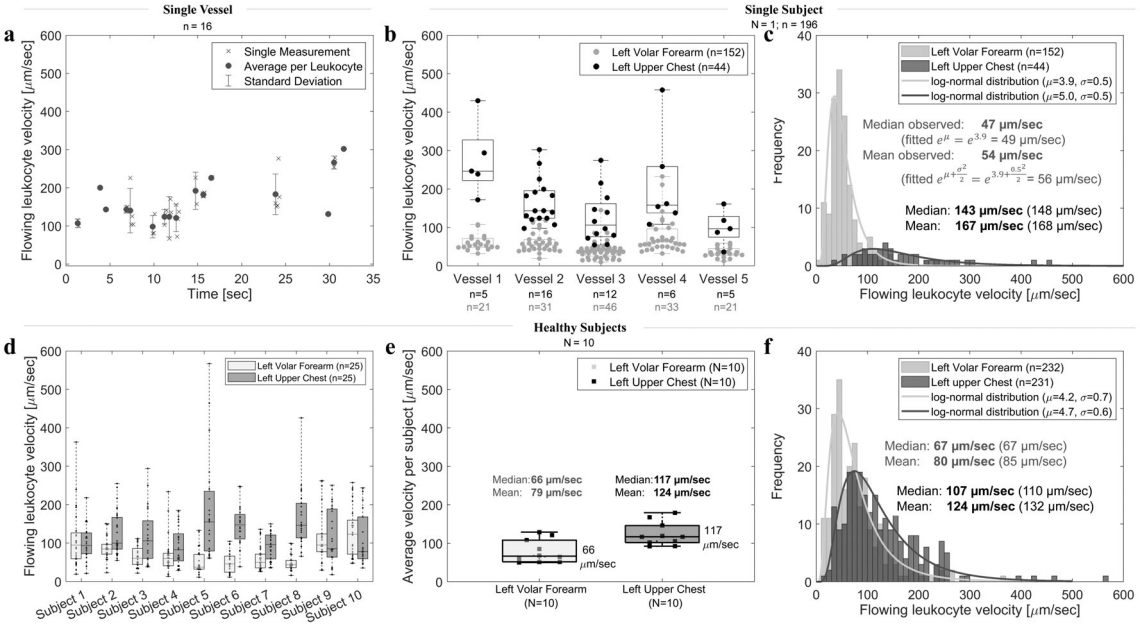

Figure 4.

Flowing leukocyte velocity variations. **(a)** Variation within a single chest vessel (vessel 2) over the course of 30 seconds. Average velocity per leukocyte was calculated from 2–5 single measurements (represented by x) of the same leukocyte in consecutive frames. **(b)** Variation among 5 nearby vessels within the same 8×8 mm^2 imaging area of subject 5. Each dot represents average velocity of a single leukocyte. **(c)** A histogram of all leukocyte velocities in the forearm and chest of a single subject (subject 5); median and mean velocity values of all measurements (observed) and calculated from the fitted log-normal distribution (in brackets). **(d)** Variation among 10 healthy subjects. Each dot represents a single leukocyte. Velocities of 5 leukocytes in 5 vessels per site were evaluated, resulting in 25 velocities per site per subject. **(e)** Variation among mean and median velocity per all subjects. Each square represents the average velocity per subject (N=10). **(f)** A histogram of all measured leukocyte velocities (n=232 in the forearm, n=231 in the chest) in all 10 healthy subjects. Note that in all graphs N represents the number of subjects (squares), whereas n represents the number of leukocytes (dots).

Table 1.

Leukocyte size comparison: undeformed (measured in isotonic solution)[14] versus as measured on a blood smear[17].

Blood cell	Cell diameter [μm]	
	Undeformed[14]	Blood smear[17]
Lymphocyte	4–8	6–15
Neutrophil	5–8	15–18
Monocyte	4–10	15–20
Eosinophil	6–8	14

Table 2.

Video acquisition protocol by laser confocal video microscopy.

1	Attach the VivaScope 1500 to the selected skin area of interest.
2	Move to the depth with visible capillaries, typically, at the DEJ or slightly below (~50–80 μm below the skin surface).
3	Move in the x-y plane within the total FOV (8×8 mm^2) to select a 0.5×0.5 mm^2 area with presence of at least one capillary with (a) a clearly visible blood flow, and/or (b) adherent or rolling leukocyte.
4	Move along the z axis to select a depth where blood flow and/or an individual leukocyte is most clearly visible (blood cells are in focus).
5	Take a 30-second video.
6	Repeat steps 4–7 to collect ten 30-second videos per imaging site. Cover different areas of the total FOV.

Table 3.

Nine quantitative parameters characteristic of the upper dermal microvasculature of human skin: comparison of median values between two body sites in ten healthy subjects (N=10).

	Parameter	Definition	Median [IQR][1] (N=10)	
			Left Volar Forearm	Left Upper Chest
1	*Density of Blood Vessels*	Number of blood vessels per 0.5×0.5 mm^2 area	2 [2–3]	2 [2–2]
2	*Flow Width*	Lower bound of true blood vessel size	5 [4–6] μm	5 [4–5] μm
3	*Interconnective Tissue Width*	Upper bound of true blood vessel size	16 [12–17] μm	14 [12–14] μm
4	*Flowing Leukocyte Velocity*	Flowing leukocyte: freely flowing with the rest of the cells	66 [52–108] μm/sec	117 [102–146] μm/sec
5	*Number of Adherent Leukocytes*	Adherent leukocyte[56]: stationary for 30+ seconds	1.5 [0–3]	0 [0–1]
6	*Number of Rolling Leukocytes*	Rolling leukocyte: rotating along the vessel wall	0	0
7	*Number of Paused Leukocytes*	Paused leukocyte: temporarily stopping, coinciding with the simultaneous stopping of the blood flow	1 [0–2]	0 [0–2]
8	*Time of Leukocyte Being Paused*	The amount of time the leukocyte and the blood flow stop for	7 [2–12] sec	3 [2–17] sec
9	*Flowing Leukocyte Size*		6 [6–7] μm	7 [5–8] μm
	Adherent Leukocyte Size		8 [7–9] μm	8 [8–9] μm
	Paused Leukocyte Size		7 [6–8] μm	7 [5–9] μm

[1]The median is calculated from 10 videos, 5 minutes of video per each site. IQR = interquartile range.